COMPARISON OF 1998 AND 1999 LEONID LIGHT CURVE MORPHOLOGY AND METEOROID STRUCTURE

IAN S. MURRAY AND MARTIN BEECH
Department of Physics, University of Regina, Regina, Saskatchewan, CANADA S4S 0A2
E-mail: murray1i@mail.uregina.ca

MICHAEL J. TAYLOR
Space Dynamics Laboratory, Utah State University, Logan, Utah 84322-4145, USA

PETER JENNISKENS
SETI Institute, NASA ARC, Mail Stop 239-4, Moffett Field, CA 94035, USA

and

ROBERT L. HAWKES
Mount Allison University, Physics Department, 67 York St., Sackville, New Brunswick, CANADA E4L 1E6

(Received 27 June 2000; Accepted 14 July 2000)

Abstract. Photometric low-light level video observations of 1999 Leonid storm meteors have been obtained from two airborne platforms during the Leonid multi-instrument aircraft campaign (Leonid MAC). The 1999 Leonid light curves tend to be skewed towards the end point of the trajectory, while the 1998 Leonid light curves were not. The variation in the light curves from 1998 and 1999 can be explained as an overall reduction in the mass distribution index, α from ~ 1.95 in 1998 to ~ 1.75 in 1999. We have interpreted this behaviour as being either indicative of a gradual loss of the "glue" that keeps the grains together, or the fact that the meteoroids sampled in 1998 had a different morphological structure to those sampled in 1999. The early fragmentation of a dustball meteoroid results in a light curve that peaks sooner than that predicted by classical single body ablation theory.

Keywords: Comets, dust, Leonids 1999, lightcurves, meteoroids, meteors

1. Introduction

Until the various *in situ* cometary rendezvous, dust sample and return missions presently underway and planned are completed, we must infer the physical and chemical properties of large (> 50 micron) cometary meteoroids through their interactions with the Earth's atmosphere as meteors. This paper is concerned with the morphology of dust from comet 55P/Tempel-Tuttle, as it was measured from light curve characteristics during the 1998 and 1999 Leonid MAC (Jenniskens, 1999; Jenniskens *et al.*, 2000).

The light that constitutes the passage of a meteor is produced through collisions between ablated meteoric atoms and atmospheric molecules. In the case of small meteoroids the light produced is assumed to be proportional to the rate of change in its kinetic energy. Also, since the velocity remains approximately constant over the luminous trail, the light produced is proportional to the rate of change of meteoroid mass. As a consequence of the rapid atomic excitation and decay process, the light produced gives a direct indication of the instantaneous rate of ablation. The dimensions of the meteoroids studied in this work (typically hundreds of μm) are much less than the mean free path at the heights of atmospheric ablation, and therefore the interaction between the atmosphere and the meteoroid is essentially molecular, with no air cap or shock wave formation.

A solid, compact, non-fragmenting meteoroid will produce a classical light curve with the point of maximum luminosity appearing near the end of the trail (Cook, 1954; Öpik, 1958; McKinley, 1961). The classical light curve reflects both the exponential increase of air density with decreasing altitude and the accelerated decrease in meteoroid surface area at the end of the trajectory. Faint television meteors have been found to have light curves that are on average nearly symmetrical (Hawkes *et al.*, 1998; Fleming *et al.*, 1993; Campbell *et al.*, 1999; Murray *et al.*, 1999). In order to explain such behaviour, we will use the dustball meteoroid ablation model developed by Hawkes and Jones (1975). In this model meteoroids are pictured as a collection of silicate and metallic grains bonded together by a secondary low-boiling point "glue". In this paper we will consistently refer to the sub-units of a meteoroid as grains, and reserve the word meteoroid for the entire solid object. Several authors (Hapgood *et al.*, 1982; Beech, 1984; 1986) have successfully applied the Hawkes and Jones (1975) model to the Perseid,

Draconid, and α-Capricornid meteor showers. Here the dustball model has been expanded to include a description of the mass distribution of grains in a meteoroid. A distribution in the masses of the constituent grains results in an overall light curve that is broader and is earlier skewed than that produced by a classical light curve (Campbell, 1999).

During the 1998 Leonid Multi-Instrument Aircraft Campaign, we measured light curves of a sample of Leonid meteors and described the asymmetry of the light curves, many of which were skewed towards the early part of the trajectory (Murray *et al.,* 1999). We have now measured a sample of light curves from the 1999 Leonid storm under similar conditions and find a quite different behaviour.

2. Experimental Observations

The experimental conditions in this study were similar to those during the 1998 Leonid MAC (Murray *et al.*, 1999). Two co-aligned intensified cameras were pointed at a constant elevation angle of 75^{o} out of a high window port on the FISTA (Flying Infrared Signature Technologies Aircraft). This time, however, both cameras were synchronised using an AC coupling feature of the individual camera systems; this allowed for accurate synchronous frame information to be obtained. Also, one of the two cameras, designated N, was equipped with a narrow band (bandwidth: 50% transmission at 8.96 nm and 10% at 13.03 nm) sodium filter centred at 589.50 nm. With peak transmittance of 64%, the filtered camera reached a limiting apparent stellar magnitude of approximately +4.0.

In parallel with these measurements, narrow field observations were made from the ARIA (Advanced Ranging Instrumentation Aircraft) using two co-aligned Xybion intensified video cameras mounted at an elevation of ~30° on the starboard side of the aircraft. One camera, type RG-350 fitted with a GEN III image intensifier, had a spectral range of ~350-900 nm and was fitted with a variety of filters during the night of the storm including two narrow band interference filters; one centered on the magnesium emission at ~520 nm and the other on the sodium emission at 589 nm. Both filters had a bandwidth of 10 nm (full-width at half maximum) and a peak transmission of ~50%. This imager was fitted with a 75 mm, f/1.4 lens (field of view 8° x 7°) and well over 200 meteors were recorded at various emission wavelengths of which 43

were imaged using the Na and Mg filters. To aid the interpretation of these data simultaneous "white-light" video observations were also made using a wider field of view (23° x 18°) GEN II intensified Xybion camera. However, this system developed an intermittent fault during the mission and the data are only suitable for pointing registration. Additional white-light observations were obtained with wide angle (39° x 28°) for cameras used for flux measurements (Jenniskens *et al.*, 2000). Video imagery from ARIA was recorded onto NTSC standard Hi-8 tapes. A time-date signal was also added to the audio track of each videotape to enhance timing analysis studies.

3. Light curve symmetry

The data were analysed as before (Murray *et al.*, 1999). The meteor images were calibrated to an apparent magnitude scale using a number of background stars. The peak brightness and integrated brightness were determined. The integrated brightness was then converted to photometric mass. The results are presented in Table I. Columns give the camera M photometric results. Maximum luminosity is the brightest recorded point expressed in astronomical magnitudes. The photometric mass is based upon an integration of the observed light curve and is expressed in kilograms. The skew parameter F is an average over the five computed values. The last three columns indicate if the beginning (B), maximum luminosity (M) and end (E) point of the meteor trail occurs in (1) or outside (0) the field of view.

All meteors in Table I are Leonids, determined by using a test for radiant match and angular velocity. Their photometric light curves are shown in Figure 1, and are normalised in intensity and duration to 'draw-out' their overall morphology. The light curves tend to have a fairly sharp rise to a rounded somewhat "flat toped", right-of-centre skewed maximum. This behaviour differs from our Leonid observations of 1998, when the light curves tended to be peak towards the beginning of the trajectory. We observed only a few exceptions to this "flat topped" or symmetrical nature. Two curves, for example, showed a double humped profile (see the 01:38:40 and 01:57:57 light curves in Figure 1). Two other light curves (see the 00:52:16 and 01:53:47 light curves in Figure 1) have characteristics that can be associated with nebulous meteors (LeBlanc *et al.*, 2000).

TABLE I

Time (UT)	Maximum Luminosity (0^M)	Photometric Mass (kg)	$F_{average}$	B	M	E
00:04:07	3.2	1.1×10^{-6}	0.76	0	1	1
00:21:21	4.5	1.6×10^{-7}	0.51	1	1	1
00:47:39	4.4	2.9×10^{-7}	0.74	1	1	1
00:47:47	5.7	3.3×10^{-8}	0.74	0	1	1
00:52:16	3.5	1.1×10^{-6}	0.79	1	1	1
00:56:21	3.6	6.5×10^{-7}	0.37	1	1	1
01:07:36	3.9	3.8×10^{-7}	0.65	1	1	1
01:10:57	4.4	1.9×10^{-7}	0.57	1	1	1
01:17:28	5.8	2.9×10^{-8}	0.79	1	1	1
01:22:00	3.5	4.3×10^{-7}	0.58	1	1	0
01:29:00	3.6	4.8×10^{-7}	0.56	1	1	1
01:32:13	4.2	2.6×10^{-7}	0.57	1	1	1
01:37:01	4.4	1.5×10^{-7}	0.49	1	1	1
01:37:33	3.8	3.2×10^{-7}	0.52	0	1	1
01:38:40	5.7	6.1×10^{-8}	0.54	1	1	1
01:38:48	3.8	3.8×10^{-7}	0.63	0	1	1
01:41:38	3.8	4.0×10^{-7}	0.81	1	1	0
01:43:14	5.0	1.0×10^{-7}	0.68	1	1	1
01:45:57	3.9	2.8×10^{-7}	0.63	0	1	1
01:49:48	6.0	2.6×10^{-8}	0.76	0	1	1
01:51:03	4.2	1.5×10^{-7}	0.65	1	1	1
01:51:05	4.5	1.9×10^{-7}	0.84	1	1	1
01:53:47	4.1	5.2×10^{-7}	N.V.	1	1	0
01:54:36	2.7	1.4×10^{-6}	0.56	1	1	1
01:57:57	4.0	3.1×10^{-7}	0.71	1	1	0
01:58:59	4.0	2.8×10^{-7}	0.46	1	1	1
02:01:45	3.6	6.7×10^{-7}	0.72	1	1	1
02:10:38	2.9	1.1×10^{-6}	0.54	1	1	1
02:11:52	2.8	1.3×10^{-6}	0.69	1	1	1
02:12:49	3.0	9.5×10^{-7}	0.69	0	1	1
02:13:41	3.2	1.0×10^{-6}	0.59	1	1	1
02:15:46	4.2	1.5×10^{-7}	0.56	1	1	1
02:16:22	3.8	3.9×10^{-7}	0.58	1	1	1
02:18:20	6.1	2.3×10^{-8}	0.14	1	1	1
02:19:27	5.0	9.2×10^{-8}	0.51	1	1	1
02:21:29	4.8	7.9×10^{-8}	0.30	0	1	1
02:22:42	3.5	5.4×10^{-7}	0.57	1	1	0
02:25:50	3.7	4.9×10^{-7}	N.V.	1	1	1
02:32:22	3.6	4.1×10^{-7}	0.40	1	1	1
02:56:12	2.6	1.5×10^{-6}	0.67	1	1	1
02:56:27	3.5	6.5×10^{-7}	0.82	1	1	1
03:01:42	3.8	3.0×10^{-7}	0.73	1	1	1
03:09:59	4.3	1.8×10^{-7}	0.63	1	1	1
03:31:26	3.6	4.8×10^{-7}	0.42	0	1	1
04:07:10	5.5	4.8×10^{-8}	0.54	1	1	1
04:12:45	3.7	3.5×10^{-7}	0.71	1	1	1
04:21:59	3.6	5.4×10^{-7}	0.72	1	1	1
04:52:00	3.7	3.6×10^{-7}	0.55	1	1	1

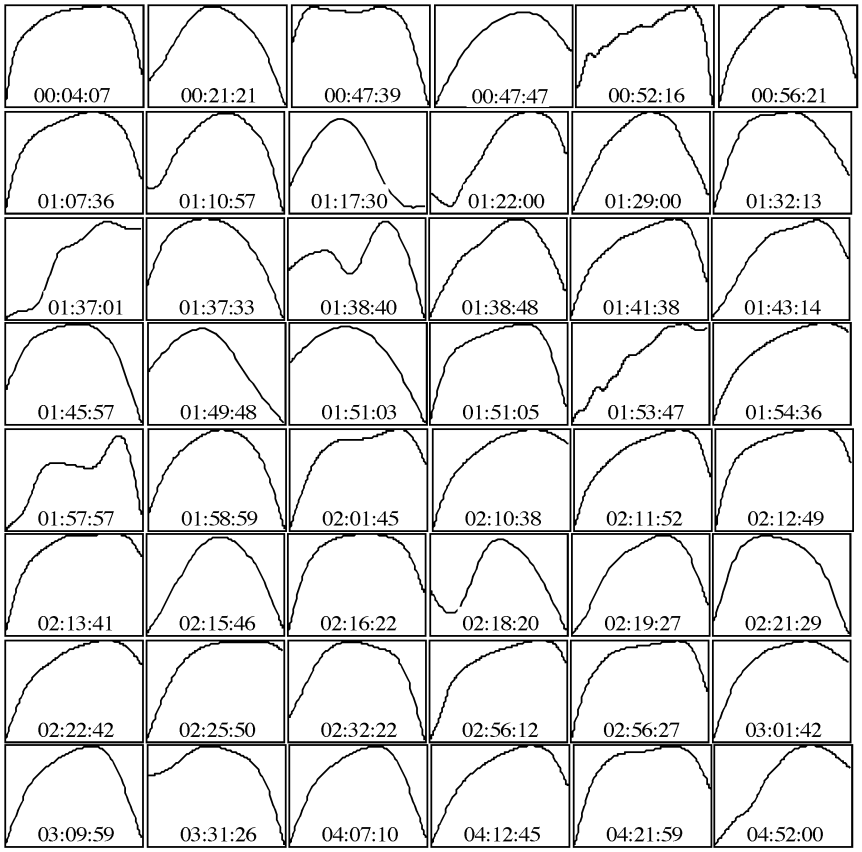

Figure 1. Photometric light curves for Leonid meteors observed with camera M. The vertical axis is a relative scale proportional to the peak magnitude and the horizontal axis is a relative time scale. The curves shown are smooth fits to the data points collected at time steps of $1/30^{th}$ of a second (the standard video frame rate).

As before, we performed a statistical analysis of the light curve profiles. The F parameter listed in Table I essentially quantifies the nature of a light curve's skew (the relative position of maximum). The F-parameter is defined as the ratio of the distance to the point of maximum brightness to the entire length of the curve (see e.g., Fleming *et al.*, 1993; Murray *et al.*, 1999):

$$F_{\Delta m} = \frac{t_{B\Delta m} - t_{MAX}}{t_{B\Delta m} - t_{E\Delta m}} \qquad (1)$$

where t_{max} is the time of light curve maximum and $t_{B\Delta m}$ and $t_{E\Delta m}$ are the beginning and end times at which the brightness is Δm magnitudes fainter than the maximum. The F-values were calculated at magnitude intervals of Δm equal to 0.25, 0.50, 0.75, 1.0 and 1.25 fainter than maximum brightness. The F-values where then averaged to give the values listed in Table I.

TABLE II

	Camera System	$F^*_{0.25}$	$F_{0.50}$	$F_{0.75}$	$F_{1.00}$	$F_{1.25}$
Mean	50mm 1999	0.58	0.61	0.62	0.63	0.61
Std. Dev.		0.17	0.15	0.15	0.14	0.15
Mean	50 mm 1998	0.46	0.45	0.48	0.47	0.49
Std. Dev.		0.20	0.18	0.14	0.15	0.14

*) Mean F-values for the Leonid light curves sampled in 1998 (penultimate row) and 1999 (first row).

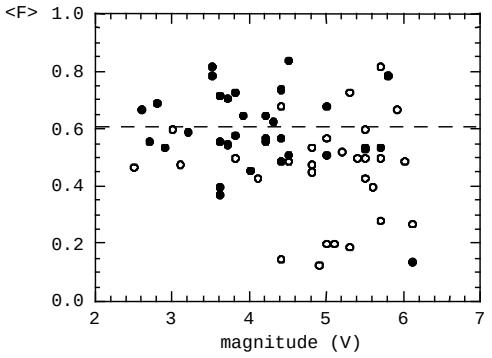

Figure 2. The F-parameter as a function of peak brightness of the meteors. Dashed line shows the mean F value for a classical light curve while (o) and (•) designate 1998 and 1999 data points.

The result of averaging the F-values for all of the sampled light curves (Table II) is a mean of 0.61, essentially the value expected for a classical light curve with a peak occurring towards the end of the trajectory. A perfectly symmetric light curve will have an F-value of 0.5 for all Δm; a light curve with an early maximum will have $F < 0.5$; a late maximum will have $F > 0.5$. However, this result is somewhat misleading since the

F-parameter fails to account for the 'flat-topped' nature of the light curves and in general the light curves of Figure 1 are not well represented by the classical curve. It is important to note, however, that the 1998 Leonid meteors showed a skew towards the early part of the trajectory, with a mean F of 0.47 (Murray *et al.*, 1999).

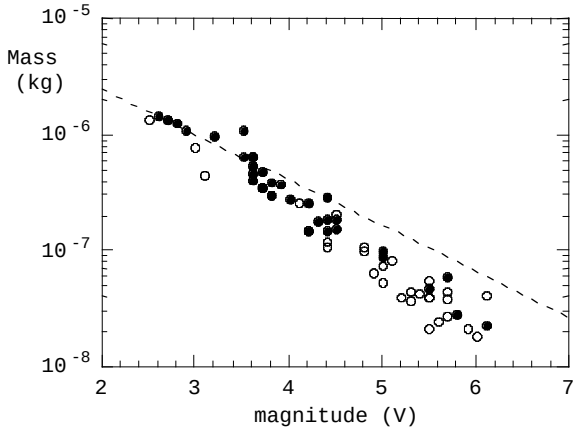

Figure 3. The integrated light curve as reflected in the photometric mass calculation versus the peak brightness. Here the dashed line is the expected relationship, while (o) and (•) designate 1998 and 1999 data points respectively.

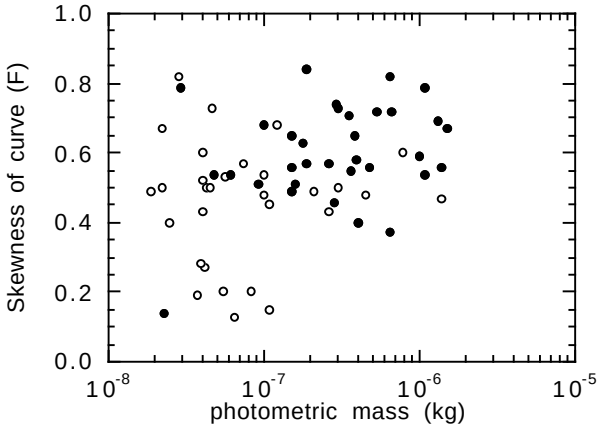

Figure 4. The F-parameter as a function of photometric mass. Where (o) and (•) designate 1998 and 1999 data points.

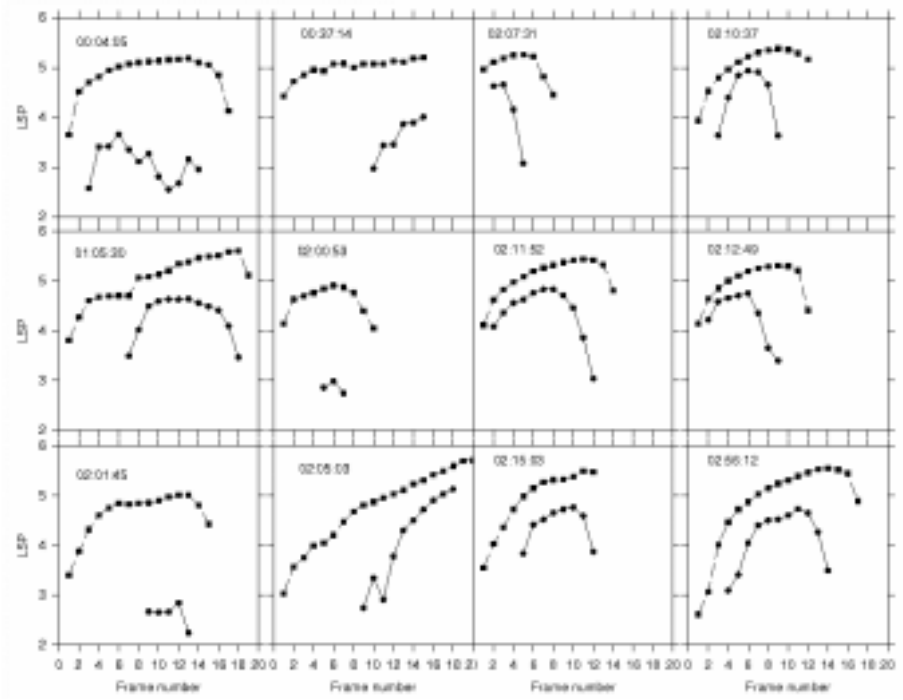

Figure 5. Comparison of the sodium filtered and unfiltered light curves for 12 Leonid meteors. In each diagram the Na light curve is always the lower of the two displayed. In this diagram the vertical axis corresponds to the log sum pixel (LSP) count and the horizontal axis is a relative time scale showing individual sequential video frames. Each frame is separated by a time interval of $1/30^{th}$ of a second. The filled circles and squares are individual data points.

Figure 2 shows the skew (averaged F-values) of both 1998 and 1999 light curves as a function of the peak brightness. A trend towards lower F values for the 1998 light curves is apparent in Figure 2. Seven light curves from 1998 have $F < 0.4$, while only 2 from 1999 are smaller than 0.4. Four light curves from 1998 have $F > 0.6$ while 14 of the 1999 light curves have averaged F-values larger than 0.6. The difference in the light curves also shows up in the calculated photometric masses. For a given peak brightness, the 1998 meteors have a smaller integrated intensity (photometric mass) as shown in Figure 3. The dashed line in Figure 3 shows the expected relationship if all the meteor light curves are identical and a constant fraction of the kinetic energy is transformed into light (this assumption implies $\log M \sim 0.4 m_v$). When plotting the F-

parameter as a function of photometric mass (Figure 4), we notice that neither data set shows a mass-dependence. However, the 1999 data are mostly displaced to higher F-values and higher photometric masses.

4. Sodium Filtered Light Curves

An important clue to the fragmentation and ablation properties of the Leonid meteoroids is differential ablation, where one mineral evaporates earlier than another. Borovicka *et al.* (1999) have argued that several of the fireballs observed during the November 1998 Leonid display exhibited evidence for the early depletion of sodium. Building upon this result, we have extended the analysis of sodium depletion to fainter Leonid meteors.

Our procedure has been to compare the light curves of simultaneously observed meteors. That is, we have obtained the simultaneous light curves of Leonid meteors at visual wavelengths and through a narrow band sodium filter. A total of 12 Leonid meteors imaged from FISTA proved to be bright enough (brighter than the approximately +4 limiting magnitude of the sodium filter camera) for a comparative analysis. Accurate timing information and the synchronised nature of the two camera systems allowed for frame-by-frame comparisons of the unfiltered (visual) and filtered images. This capability allows for a straightforward log sum pixel comparison of the observed light curves.
The visual and Na light curves are shown in Figure 5. Note that the 00:37:14 and 02:05:03 events show only the beginning part of the meteor. Much variability is observed between individual Na light curves.

We seemingly confirm the discovery by Borovicka *et al.* (1999) that sodium is depleted before all ablation has stopped. Typically the sodium light curve falls off sooner than its visual counterpart. Also, we notice that the sodium curves have a later onset than the visual light curves. This suggests the Na-rich phases are not part of the meteoroid "glue" but belong to the grain component.

The relative intensity of sodium and white light emission varies considerably from one light curve to the next. From Figure 5 it appears that the stronger sodium signal is observed for light curves with the steepest increasing slope, or the highest F value. This result, however, will require further study and modelling.

An initial investigation of the sodium and magnesium light curves recorded with the ARIA filtered camera was performed to determine

their overall morphology. As first indicated by Borovicka *et al.* (1999) one might expect to find systematic differences between the light curves observed through sodium and magnesium filters. This situation can arise because sodium and magnesium reside in different host phases in IDPs (Rietmeijer, 1998; 1999; 2000) and meteorites (Papike, 1998). To date 14 complete (5 magnesium filtered and 9 sodium filtered) Leonid light curves have been examined (see the scaled sequence of light curves in Figure 6).

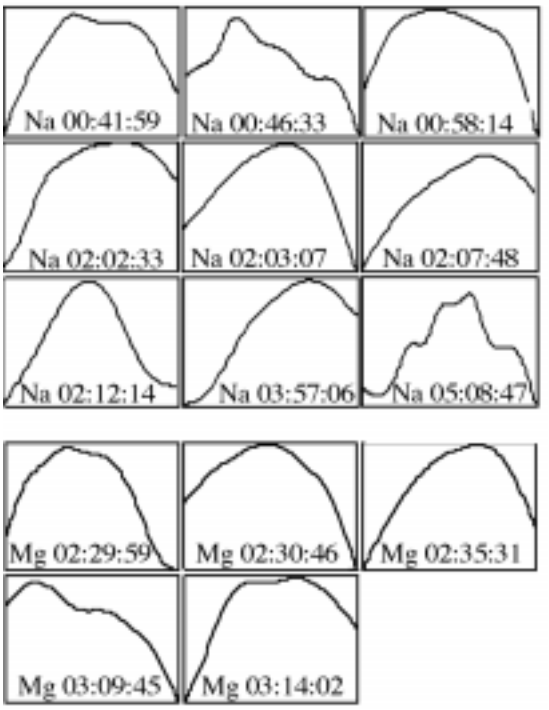

Figure 6. Nine calibrated filtered Na (top) and five Mg (bottom) light curves from the ARIA observations. As with the earlier presented light curves, they are plotted with relative scales to show overall morphologies.

We find that, in general, the morphology of the filtered light curves is similar to those shown by the non-filtered observations (see Figures 5). Some sodium light curves show significant intensity variations along the meteor trajectory. Although low number statistics prevail, F-values were computed for the ARIA filtered light curves at log sum pixel intervals

equivalent to apparent magnitude intervals of $\Delta m = 0.2, 0.4, 0.6, 0.8$ and 1.0. Mean values for the five intervals considered result in an average F-value of 0.55 for the magnesium filtered light curves and an average F-value of 0.50 for the sodium filtered light curves.

5. Dustball model calculations

Since we have at present no clear knowledge of how Leonid meteoroids are 'constructed', we shall assume for modelling purposes a mass distribution for which the number of constituent grains, with masses between m and m + dm, is proportional to $m^{-\alpha}$, where α is the mass distribution index. In this fashion, by fixing upper and lower mass limits on the constituent grains present, we may 'build-up' any given initial mass Leonid meteoroid by adding together the appropriate numbers of component grains. The modelling discussed here considers twelve fundamental grain masses; the largest grains have masses of 10^{-7} kg, while the smallest grains have masses of 5×10^{-13} kg. The mass range adopted for the fundamental grains is somewhat arbitrary, but reflects the range of grain masses deduced from observed flare events in large, bright meteors (Smith, 1954; Simonenko, 1969; Campbell *et al.*, 1999). In general we note, that the smaller the value of the mass distribution index the greater the relative number of 'large' grains; the larger the mass distribution index the greater the relative number of 'small' mass grains.

The dustball model that we have constructed follows the classical, single-body ablation of individual grains and determines the variation in light intensity as a function of initial mass and atmospheric height. We assume that all of the grains have the same 'generic', that is stone-like composition as specified by Fyfe and Hawkes (1986) and used by Campbell *et al.*, (1999). The single-body ablation equations for mass loss and deceleration are solved numerically with atmospheric density being interpolated from the MSIS-E-90 Earth atmosphere model. The instantaneous luminous intensity, *I*, produced by a small single-body meteoroid is assumed to be proportional to the rate of change of its kinetic energy. The overall light curve, however, is synthesised by combining the number-weighted intensities of the constituent grains as a function of atmospheric height. Figure 7 shows a series of synthesised light curves for a 10^{-6} kg Leonid meteoroid (V = 71 km/s and a zenith angle of 45 degrees). The curves are labelled according to the assumed

mass distribution index (α). It can be seen that 'flat topped' light curves require a mass distribution index $\alpha \sim 1.8$.

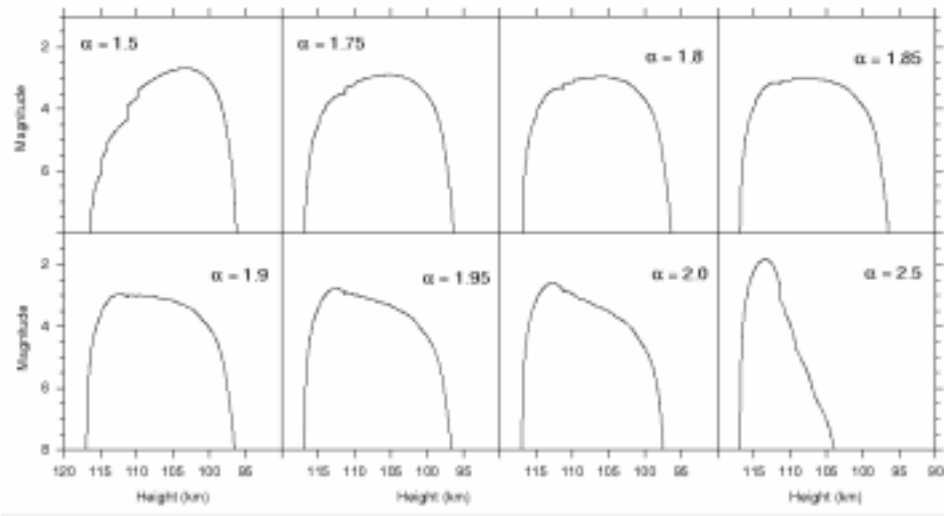

Figure 7: Synthesised light curves for a 10^{-6} kg Leonid meteoroids for a range of grain size distributions.

For small values of $\alpha < 1.5$ the synthesised light curve approaches the classical light curve of the largest mass grain. Likewise the synthesised light curves constructed with $\alpha > 2.5$ would approach that of the classical light curve of the lowest mass grain. For $1.5 < \alpha < 2.5$, a range of variable light curve morphologies are realised. We see, for example, that when $\alpha \sim 1.5$ the light curve has a near linear increase to its maximum and is late skewed. For $\alpha \sim 1.85$ the light curve is very nearly 'flat topped' and symmetrical about the maximum. For $\alpha > 1.9$ the light curve has an early peak and displays a near linear decrease of magnitude with time after the maximum. We see also from Figure 7 that there is a systematic shift in the height of the light curve maximum as α increases from 1.5 to 2.5. For $\alpha = 1.5$ the maximum is at 103.4 km altitude, at $\alpha = 2.5$ the maximum is at 113.4 km altitude (assuming a zenith angle of 45 degrees). The change in height of the light curve maximum, as a function of the mass distribution index, is at its most dramatic for $1.8 < \alpha < 1.9$. In this range the height of maximum increases by some 7 kilometres. In

principle it appears that one may be able to construct a monotonic relationship between the mass distribution index and the height of maximum for a given initial meteoroid mass – we intend to pursue the development of this idea in a subsequent publication.

Table III compares the classical single-body meteoroid of mass 10^{-6} kg, with those for several dustball meteoroids constructed with various mass-distribution indices. The F-values for a classical, single-body ablation light curve are given for comparison in the last row of the Table. We acknowledge that the F-parameter does characterise the basic change in symmetry of a light curve but note that it offers little physical information about the meteoroid. In future it will be desirable to phase out the use of the F-parameter and substitute a more physically meaningful morphological parameter (e.g. Campbell *et al.,* 1999). Still, the observed variation in the light curves from 1998 and 1999 Leonid meteor storms can be explained as an overall reduction in α from ~ 1.95 in 1998 to ~ 1.75 in 1999.

TABLE III

α	$\Delta m = 0.25$	$\Delta m = 0.50$	$\Delta m = 0.75$	$\Delta m = 1.00$
1.50	0.56	0.58	0.59	0.59
1.85	0.53	0.50	0.50	0.48
2.00	0.55	0.37	0.30	0.26
2.50	0.52	0.53	0.53	0.54
Classical	0.58	0.61	0.63	0.65

A few of the Leonid light curves observed in 1999 appear to be ‘odd’. For example the double peaked, or ‘humped’ light curves (e.g. the 01:38:40 and 01:57:57 light curves in Figure 1) do not fit the single mass distribution index scheme described above. We do not believe, however, that the second, brighter maximum shown by these meteors is due to flaring or fragmentation, but find that the light curves may be readily described as a dustball with an additional ‘massive’ grain. Figure 8 illustrates, by way of example, a synthesised light curve for the 01:57:57 light curve shown in Figure 1. We find the light curve is reasonably well described by a 2.4×10^{-7} kg dust ball constructed with $\alpha = 1.85$, and an additional single grain of mass between 2 to 2.5×10^{-7} kg.

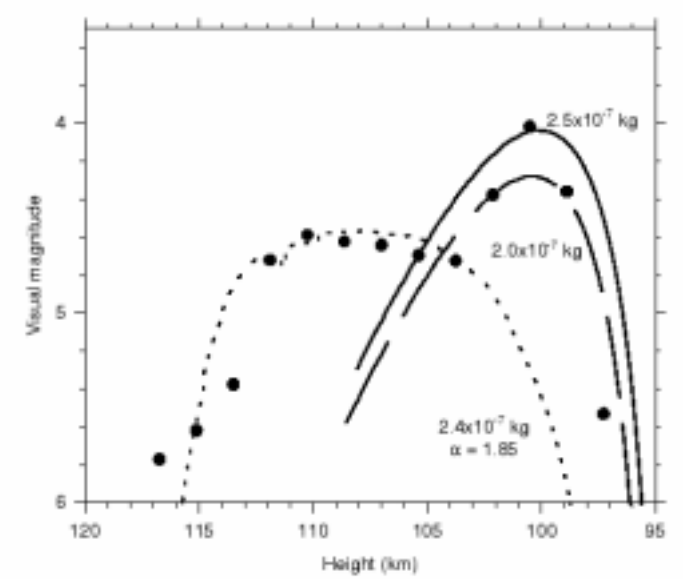

Figure 8. Composite light curve model for the 'humped' Leonid meteor observed at 01:57:54 UT, 1999 November 17. The dots correspond to the derived magnitudes. The dashed line shows the synthesised light curve for a 2.4 x 10^{-7} kg meteoroid with $\alpha = 1.85$. The solid and broken-solid lines correspond to the classical light curves for 2.0 and 2.5 x 10^{-7} kg meteoroids.

6. Discussion

The apparently higher mass distribution index α for the constituent grains of the 1998 Leonid meteoroids is highly interesting. One reason for this apparent enhancement could be that the 1998 meteoroids have a significantly different ejection age than the meteoroids sampled in other years. While the 1999 Leonid shower was predominantly composed of debris ejected in 1899 (McNaught and Asher, 1999), the material sampled in 1998 was ejected from comet 55P/Tempel-Tuttle several perihelion passages before 1899 (Asher *et al.*, 1999; Jenniskens and Betlem, 2000). If older grains dominate the 1998 Leonid sample set it would imply that meteoroids become progressively more fragmented over time during their exposure to the interplanetary environment. This effect may be mitigated through repeated heating and cooling episodes associated with returns to perihelion, and possibly the "glue" that holds the grains together may be gradually lost or made less sticky by UV

photoprocessing. Likewise, the "glue" could be modified through irradiation by energetic solar wind and solar flare nuclei, or both. It is highly probable that the 'glue' component responsible for bonding a dustball meteoroids grains together is organic in nature and compositionally it maybe similar to the CHON particles detected during the GIOTTO spacecraft encounter with comet 1P/Halley (see e.g., Jessberger *et al.*, 1988). The organic component probably produces very little luminosity in the visual and near-visual regions of the electromagnetic spectrum, and consequently it might well remain undetected with the typical equipment used to record 'visual' light curves. The height distributions of meteors observed with radar, however, have recently been interpreted by Steel (1998) and Elford *et al.* (1997) as being indicative of the fact that most meteoroids must have a high, heavy organic make-up. The low-boiling point of the constituent organic compounds makes the meteoroids susceptible to on-going fragmentation as they descend through the Earth's upper atmosphere.

Acknowledgements

We extend our many thanks to Joe Kristl who has un-begrudgingly helped with many tape-editing and copying tasks. The help and guidance of Mr. D. Prohor of the Faculty of Film and Video at the University of Regina is gratefully acknowledged. Many thanks to Mr. D. Kolybaba and Mr. K. Wolbaum of the Faculty of Science at the University of Regina for their technical assistance. Special thanks go to Andrew LeBlanc for his helpful suggestions and comments. We also gratefully acknowledge and thank the 452nd Flight Test Squadron at Edwards Airforce Base for their logistical support during the 1999 Leo MAC and the many people who have made this mission possible. This work was partially supported with funds provided by the National Science and Engineering Research Council of Canada, the Space Dynamics Laboratory at Utah State University and the US National Science Foundation grant No ATM-9612810. Leonid MAC is supported by the NASA Planetary Astronomy and Exobiology programs, the NASA Advanced Missions and Technologies Program for Astrobiology (AAMAT), and USAF/XOR. *Editorial handling*: Frans Rietmeijer.

References

Asher, D.J., Bailey, M.E., and Emelyanenko, V.V.: 1999, *MNRAS* **304**, L53–L56.

Beech, M.: 1984, *MNRAS* **211**, 617–620.

Beech, M.: 1986, *Astron. J.* **91**, 159–162.

Borovicka, J., Stork, R., and Bocek, J.: 1999, *Meteoritics Planet. Sci.* **34**, 987–994.

Campbell, M.D., Hawkes, R.L., and Babcock, D.D.: 1999, in V. Porubcan and W.J. Baggaley (eds.), *Meteoroids 1998*, Slovak Academy of Sciences, Bratislava, Slovakia, 363–366.

Cook, A.F: 1954, *Ap. J.* **120**, 572–577.

Elford, W.G., Steel, D.I. and Taylor, A.D.: 1997, *Adv. Space. Res.* **20**, 1501–1504.

Fleming, D.E.B., Hawkes, R.L. and Jones, J.: 1993, in J. Stohl and I.P. Williams (eds.), *Meteoroids and Their Parent Bodies*, Slovak Academy of Sciences, Bratislava, Slovakia, 261–264.

Fyfe, J.D.D. and Hawkes, R.L: 1986, *Planet. Space. Sci.* **34**, 1201–1212.

Hapgood, M., Rothwell, P., and Royvrik, O.: 1982, *MNRAS* **201**, 569–577.

Hawkes, R.L. and Jones, J.: 1975, *MNRAS* **173**, 569-577.

Hawkes, R.L., Campbell, M.D., Babcock, D., and Brown, P.: 1998, D. Lynch, *et al.* (eds.), *Proc. 1998 AIAA Leonid Threat Conf.* 11 pp.

Jenniskens, P.: 1999 *Meteoritics Planet. Sci.* **34**, 959–968.

Jenniskens, P. and Betlem, H.: 2000, *Ap. J.* **531**, 1161–1167.

Jenniskens, P., Butow, S. and Fonda, M.: 2000, *Earth, Moon and Planets* **82-83**, 1–26.

Jessberger, E. K., Christorforidis, A., and Kissel, J.: 1988,*Nature* **322**, 691–695.

LeBlanc, A.G., Murray, I.S., Hawkes, R.L., Worden, P., Campbell, M.D., Brown, P., Jenniskens, P., Correll, R.R., Montague, T. and Babcock, D.D: 2000,*MNRAS* **313**, L9–L13.

McNaugth R.H. and Asher D.J.: 1999, *WGN, Journal of the IMO* **27**, 85–102.

Murray, I.S., Hawkes, R.L., and Jenniskens, P.: 1999, *Meteoritics Planet. Sci.* **34**, 949–958.

McKinley, D.W.R.: 1961, *Meteor Science and Engineering*. McGraw-Hill, New York, 308 pp.

Opik, E.J.: 1958, *Physics of meteor flight in the Atmosphere.* Interscience, New York., p. 63–68.

Papike J.J (ed.), 1998; In *Planetary Materials, Reviews in Mineralogy* **36**, 1039 pp., The Mineralogical Society of America, Washington, DC, 1052 pp.

Rietmeijer, F.J.M.: 1998. in A.S. Marfunin (ed.) *Advanced Mineralogy*, **3**, Springer Verlag Berlin-Heidelberg, 22p.

Rietmeijer, F.J.M.: 1999, *Ap. J.* **514**, L125–L127.

Rietmeijer, F.J.M.: 2000, *Planetary Space Science*, in press.

Simonenko, A.N.: 1969, *Astron. Vest*. **3**, 26–35.

Smith, H.J.:1954, *Ap. J.* **119**, 438–442.

Steel, D.I.: 1998, *Astron. Geophys*. **39**, 24–26.